# Evolutionary consequences of bacterial resistance to a flagellotropic phage

**Jyot D. Antani[1,2,3,✉], Austen Theroux[1], Thierry Emonet[3,4,5], Paul E. Turner[1,2,3,6,✉]**

[1]Department of Ecology and Evolutionary Biology, Yale University, New Haven, CT 06520, USA

[2]Center for Phage Biology & Therapy, Yale University, New Haven, CT 06520, USA

[3]Quantitative Biology Institute, Yale University, New Haven, CT 06520, USA

[4]Department of Molecular, Cellular and Developmental Biology, Yale University, New Haven, CT 06520, USA

[5]Department of Physics, Yale University, New Haven, CT 06520, USA

[6]Program in Microbiology, Yale School of Medicine, New Haven, CT 06520, USA

✉ Corresponding author emails: jyot.antani@yale.edu, paul.turner@yale.edu

Keywords: flagellotropic bacteriophage, phage-bacteria interactions, bacterial flagella, evolution

## Abstract

Bacteria often rapidly evolve resistance to bacteriophages (phages) by mutating or suppressing the phage-receptors, the factors that phages first target to initiate infection. Flagellotropic phages infect bacteria by initially binding to the flagellum. Since motility is an important fitness factor that allows bacteria to efficiently explore their environment, losing flagellar function to evade infection by flagellotropic phages represents a crucial trade-off. In this study, we investigated the evolutionary responses of *Escherichia coli* when exposed to the flagellotropic phage $\chi$. Using an experimental evolution approach, *E. coli* cells were repeatedly subjected to environments rich in phage $\chi$ but selective for motility. Unlike traditional well-mixed cultures, we employed swim-plate assays to simulate spatial confinement and promote motility. Whole genome sequencing of evolved populations revealed early emergence of non-motile, $\chi$-resistant mutants with mutations disrupting motility-related genes. Motile mutants emerged in later passages, possessing mutations in the flagellin gene *fliC*. Swim-plate assays showed a diverse range of motility among these mutants, with some displaying slower, and others faster, expansion speeds compared to the ancestral strain. Single-cell tracking experiments indicated an increased

tumble bias in $\chi$-resistant mutants, suggesting an adaptive response involving altered flagellar rotation. Our findings demonstrate that motility can undergo trade-offs and trade-ups with phage resistance, shedding light on the complex evolutionary dynamics between motile bacteria and flagellotropic phages.

## Introduction

Bacteriophages (phages), viruses of bacteria, have existed alongside their bacterial hosts for perhaps billions of years. Lytic phages kill host cells during the process of virus replication, representing strong selection pressure for bacteria to evolve defenses against phages attack[1,2]. Bacteria can evolve resistance at the first line of defense- by mutating or suppressing the phage receptors on the cell surface, because phages rely on these targets to initiate infection. Phages target various structures exposed on bacterial surfaces, including transmembrane channels, saccharides, and appendages. It is thought that binding to appendages that extend beyond the cell bodies enhances the probabilistic chances that freely-diffusing phages collide with such structures to find a suitable host cell for infection[3,4].

Flagellotropic phages infect bacteria by first interacting with the bacterial flagellum[5]. Flagella are extracellular appendages that extend up to multiple cell lengths. Rotation of flagella enables planktonic motility of bacteria in aqueous media as well as their swarming motility on semisolid surfaces[6]. Obstruction of flagellar rotation is thought to be the earliest signal of surface signaling which is sensed by the bacterial cell[7–9]. Motility not only allows bacteria to efficiently explore their environments, including chemotaxis (movement in response to chemicals)[10], it also represents a determinant of relative fitness among bacterial genotypes[11] and may be considered a virulence factor for certain species of bacterial pathogens[12]. If bacteria mutate their motility apparatus to evade attack by flagellotropic lytic phages, their ability to move through the environment may be negatively affected, which represents a crucial fitness trade-off suffered by bacteria that evolve phage resistance. While bacteria and flagellotropic phages are thought to coexist in nature[5,13], the mechanisms by which bacteria evolve resistance against such phages remain poorly understood.

Here, we used experimental evolution to examine how *Escherichia coli* host cells evolve resistance against phage $\chi$, a model flagellotropic phage. Phage $\chi$ requires fully functional, rotating flagella for successful infection[14,15]. We conducted serial transfer of bacterial populations founded by MG1655, a motile strain of *E. coli*, in replicated environments containing phage $\chi$ while also selecting for cell motility. Whole genome sequencing revealed that nonmotile $\chi$-resistant mutants undergo deletions in motility and chemotaxis genes, mediated by the

transposon IS1 (insertion sequence 1). In evolved populations where some cells retained motility while gaining resistance to phage $\chi$, we identified mutations in *fliC*, the gene encoding the flagellin (flagellar filament monomer). Specifically, we observed parallel evolution across treatment populations of specific key mutations – single amino acid substitutions that affect the outer D3 domain of the flagellin. Finally, we assessed the evolutionary impact on bacterial motility by conducting swim-plate assays and single-cell tracking with the evolved and ancestral cells. This study highlights the evolutionary consequences experienced by populations of motile bacteria when attacked by a flagellotropic phage.

## Experimental Overview

Typical phage-bacteria evolution assays involve co-culturing phages and bacteria in shaking flasks with replenishment of media (through dilution-bottlenecks) every ~24 h. Flagellar synthesis and operation are energetically expensive: flagellar synthesis accounts for at least 2% and up to ~10% of the total cellular energy expenditure[16]. In shaking flasks, bacteria access fresh nutrients without the need for motility, reducing the necessity for flagellar synthesis. When an anti-flagellar evolutionary pressure such as phage $\chi$ is present, bacterial mutants with defective flagellar synthesis may emerge as an easy adaptive strategy. Natural environments are more complex: while anti-flagellar evolutionary pressures exist, bacteria also need to explore their surroundings to find nutrient-rich habitats. To simulate these conditions and encourage bacteria to retain motility, we modified the swim-plate assays to evolve *E. coli* in the presence of $\chi$-phage.

We embedded motility plates (Tryptone Broth with 0.3% agar) and a high concentration of $\chi$-phage ensuring that bacteria would frequently encounter phages while swimming: 15 µL of $10^{11}$ PFU/mL $\chi$-phage were added to 10 mL of agar in each plate. This concentration of phages was worked out by carrying out a preliminary experiment to determine a concentration at which no bacterial swim rings were observed for 24 hours. 10-fold of the determined concentration was used for the evolution assay. We inoculated 5 µL of overnight culture of MG1655 (ancestor strain for the evolution assay) in the center of the plates and incubated the plates for 24-48 h at 30 °C.

After each passage (until swim rings appeared or 48 hours passed), 10 mL of the contents in the plate were pooled into a tube, 10 mL of liquid TB was added, tube was vortexed, and 10 µL of the mixture was inoculated into the next plate (freshly made, containing phage $\chi$). Plates were returned to 30 °C incubation and frozen stock (25% glycerol) was made from the mixture. We repeated this process for 10 passages, with 10 independent replicates started from the same MG1655 ancestor genotype (**Fig 1**). Each new passage occurred after 24 hours if a motile ring of bacteria was observed. If no motile ring was present (which was the case for the first 2-3

passages), incubation continued until 48 hours. This method allowed us to determine if the bacteria growing on the plate (and resistant to $\chi$) remained motile.

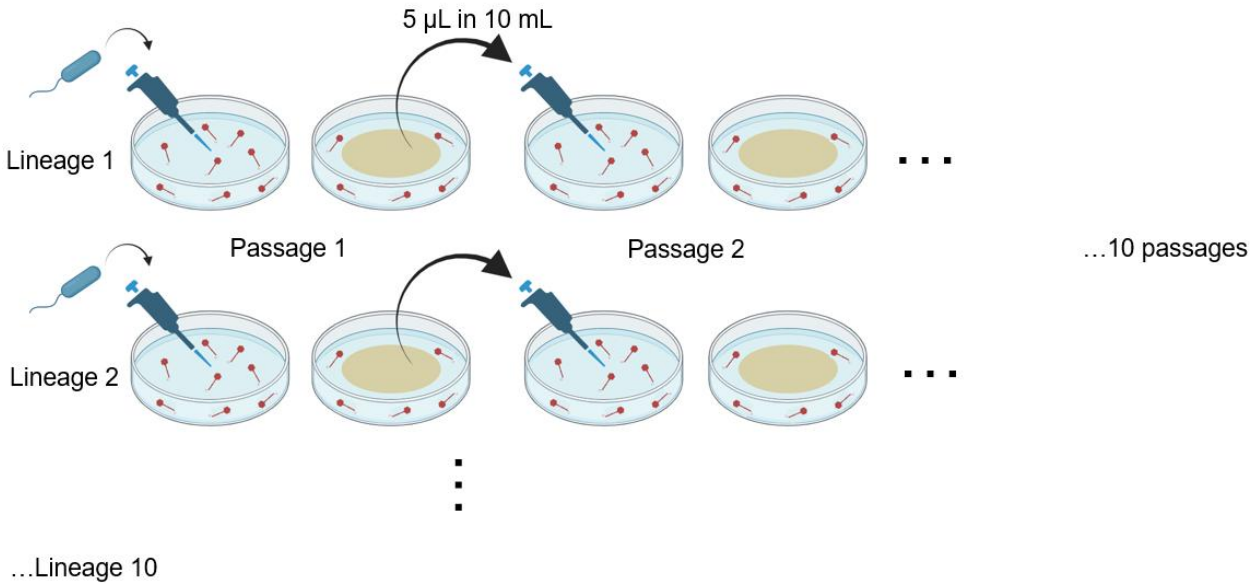


**Fig 1. Swim-plate assay for evolution of bacteria against $\chi$-phage**. We inoculated bacteria into the center of swim plates (0.3% agar) embedded with phage $\chi$. After 24-48 hours of incubation at 30 °C (a passage), we transferred an aliquot to fresh plates with $\chi$. We continued this protocol for 10 passages, for 10 independent lineages.

# Results

## Early (non-motile) mutations are mediated by insertion sequence element IS1

In early passages (up to passage 2, 3, and 4 in some cases), the bacteria did not form a motile ring even after 48 hours of incubation. Instead, non-motile cells grew on the plate as spotty colonies (**Fig 2**A). These bacteria appeared to adopt the evolutionary strategy mentioned earlier: they ceased expending energy on flagellar synthesis and rotation when subjected to $\chi$. Without functional flagella, the flagellotropic phage could not infect the cell[14,15].

To determine the mechanism behind the loss of motility, we performed whole genome sequencing on these strains. We discovered that insertion sequence element, IS1, mediates the disruption of motility-related genes. This transposon-like element is located upstream of *flhDC*, which encodes the master operon of flagellar synthesis, motility, and chemotaxis[11]. Transcription and translation of *flhDC* is essential for the downstream expression of flagellar synthesis, motility, and chemotaxis genes[17]. Analyzing the sequences through Breseq[18], we interpreted the sequencing data in the following manner: in presence of phage $\chi$, IS1 jumps downstream of *flhD*

at various locations, thus disrupting the expression of FlhDC (**Fig 2**B,C; n = 6 populations sequenced).

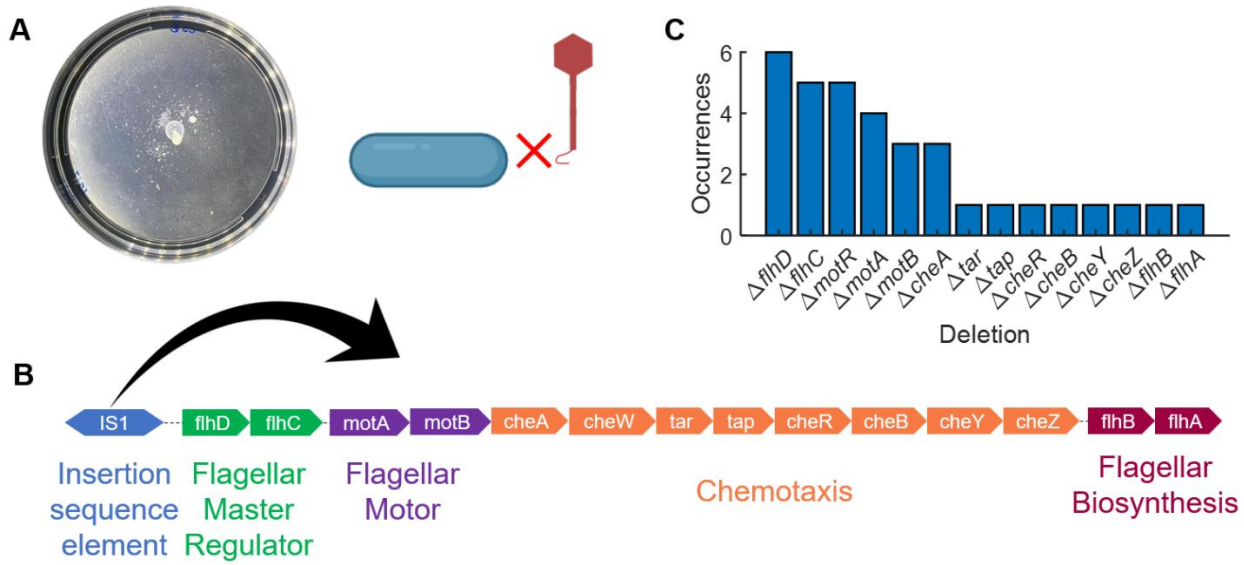


**Fig 2. Early $\chi$-resistant mutants were non-motile. (A)** In early passages (up to passage 3 or 4), bacteria developed resistance to $\chi$-phage by stopping flagellar synthesis, as $\chi$ cannot infect bacteria lacking functional flagella. The plates did not feature swim rings, instead they had spotty colonies of bacteria. **(B)** The motility-related mutations were mediated by the transposon-like insertion sequence element IS1, which is typically upstream of the flagellar regulatory genes. Transposition of IS1 disrupted the expression of FlhDC, the flagellar master operon. Whole genomes of a total of 6 mutants were sequenced, where the frequency of deletions observed is depicted in **(C)**.

## Bacteria recover motility by mutating the flagellar filament

By passages 4 or 5, we observed motility rings on the plates (**Fig 3**A), indicating that bacteria had evolved to recover motility. Interestingly, lineage 4 did not have significant growth by passage 10, which could be due to either virus-driven bacterial extinction or manual (pipetting) error. We sequenced each lineage population at passage 5 and 10, comparing their whole genome sequences with the annotated ancestral bacterial sequence to identify mutations[18]. Genes with mutations occurring at frequencies greater than 10% in these passages are listed in **Table S1** (passage 5) and **Table S2** (passage 10). Notably, several of these genes are involved in chemotaxis or flagellar machinery or the regulation of flagellar motility (highlighted in maroon). Mutations that occurred at frequencies >70% are shown in **Fig S1**. A large number of high-frequency mutations were found in *fliC*, the gene encoding the flagellin protein, which forms the flagellar filament monomer (**Fig 3**B, **Fig S1**).

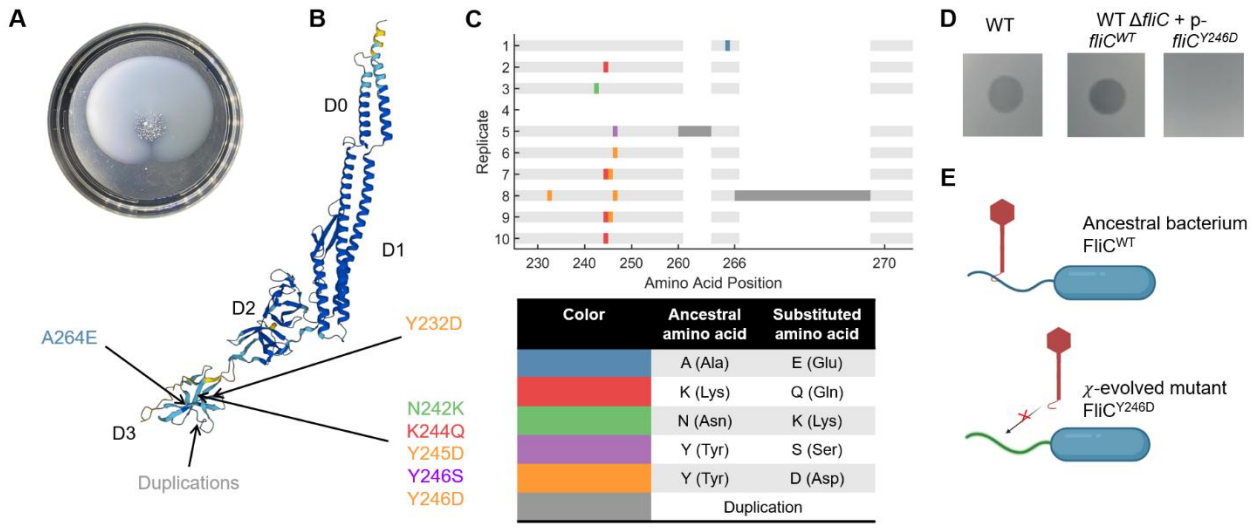


**Fig 3. Bacteria recovered motility by mutating the flagellar filament. (A)** Rings of swimming bacteria were observed in the later passages. **(B)** Structure of *E. coli* FliC (UniProt P04949) is shown with regions D0, D1, D2, and D3. All the observed *fliC* mutations encoded parts of the D3 domain. **(C)** Mutated amino acid positions in FliC are indicated for each lineage, with the color code described at the bottom. Dark grey corresponds to amino acid sequences that were duplicated. **(D)** Phage $\chi$ forms characteristic clearing on wildtype cells as well as cells with a *fliC* knockout carrying WT *fliC* on a plasmid ("p" = pTrc99A). However, Δ*fliC* cells carrying single amino acid substitution Y246D in FliC are resistant to $\chi$. **(E)** These results propose a mechanism where $\chi$ cannot bind to the mutated flagellum.

We isolated single mutants from each lineage at passage 10 and performed Sanger sequencing on *fliC*. Sequencing results from isolates within the same lineage were identical, so we present them as the consensus results for each lineage (**Fig 3**B, C). Most mutations were single or dual amino acid (AA) substitutions, all in the outermost D3 domain of the flagellin, which remains exposed on the outer surface of the flagellar filament after polymerization[19]. Given that flagellar point mutations are known to have significant effects[20], we hypothesized that a single amino acid substitution might confer resistance to $\chi$. To test this, we knocked out the *fliC* gene and expressed either FliC with AA substitution Y246D (observed in more than one $\chi$-resistant mutants) or wildtype FliC (as control) via a leaky expression vector pTrc99A. We spotted $\chi$ onto lawns of each of these strains, observing clearing (indicating bacterial infection) for cells expressing WT FliC but not those expressing FliC$^{Y246D}$ (**Fig 3**D). These results suggest that an amino acid substitution in the flagellin's D3 domain obstructs the binding of $\chi$, rendering the bacteria resistant to the phage (**Fig 3**E).

## $\chi$-resistance trades off and trades up with motility

With evolution, two traits may trade-off, trade-up, or may have neither relationship[21,22]. Since $\chi$ uses the motility apparatus, and we observed mutations in the flagellar filament which powers motility, we asked whether motility trades up or trades off with evolution of $\chi$-resistance. We performed swim plate assays to compare the swim ring diameters of the ancestral bacterial strain and isolates from passage 10 of our evolution experiments. Additionally, we evolved four ancestral lineages on swim plates without $\chi$ for 10 passages as controls. We found that six out of the nine $\chi$-resistant lineages had swim-ring diameters smaller than those for ancestors, after a 15-hour incubation, indicating evolutionary trade-off between motility and phage-resistance (**Fig 4**A). One lineage (lineage 1) expanded faster than the ancestral strain but similar to the control strains. Two lineages expanded faster than the control strains (lineages 2 and 10), demonstrating improved motility along with phage-resistance, which is an example of a trade-up (**Fig 4**A).

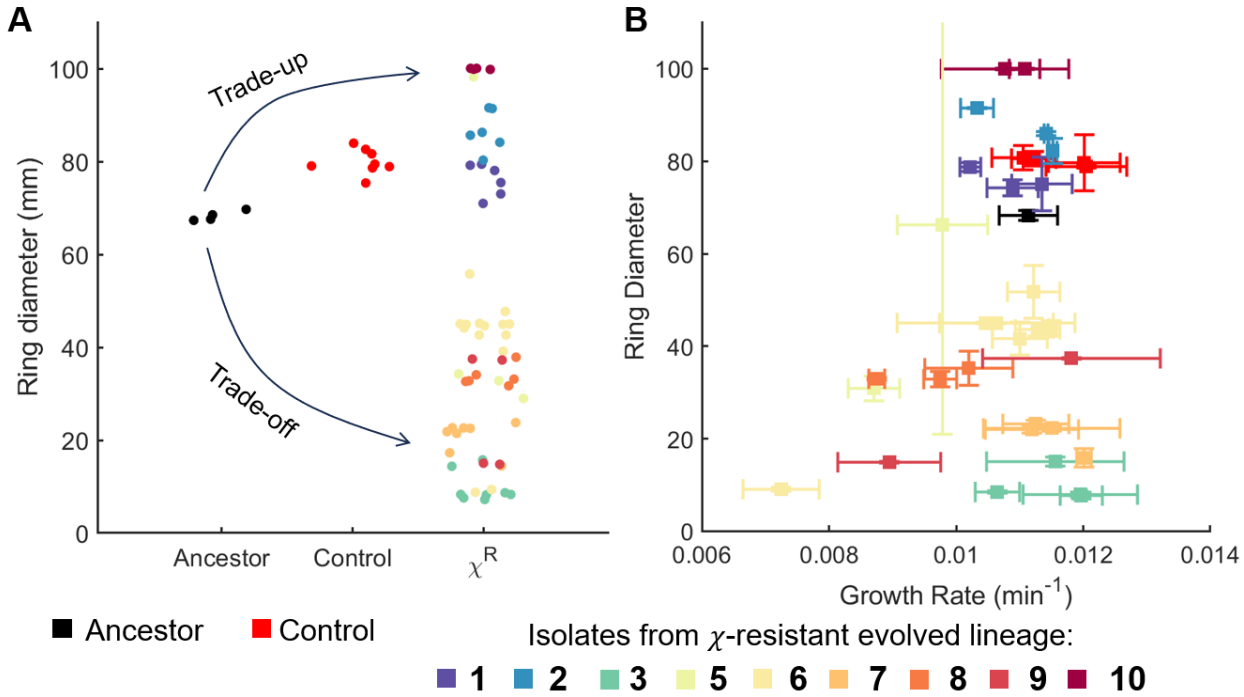


**Fig 4. Resistance to phage $\chi$ trades off as well as trades up with motility. (A)** Diameters of swim rings made by cells of ancestor (unevolved WT), controls (WT evolved in absence of phages), and $\chi$-resistant (WT evolved in presence of $\chi$) strains. The swim plates (0.3% agar) did not contain any $\chi$. Each dot represents swim diameter of an individual isolate from passage 10. We thus observe instances where motility trades off with phage-resistance and where motility is improved upon gaining phage-resistance (indicated by arrows). **(B)** Growth rate of each bacterial strain was measured and plotted against the ring diameter. These observations were uncorrelated (Pearson correlation coefficient, $\rho$ = 0.19, P-value = 0.26).

In an expanding ring of motile bacteria, both growth and chemotaxis play significantly influence the expansion speed[11,23–25]. Recent studies have shown that growth rates greatly affect expansion speeds[11,26,27]. To determine whether the differences observed in swim ring diameters can be attributed to varying growth rates, we measured the growth rates of the isolates in the microplate spectrophotometer. We plotted the swim-ring diameter of each strain against its growth rate (**Fig 4**B). These measured quantities showed no significant correlation (Pearson correlation coefficient $\rho$ = 0.19, P = 0.26), indicating that changes in growth rate is not the primary factor influencing the swim ring diameter in our experiments.

Instead, mutations in flagellar filament (**Fig 3**) and other related genes (**Fig S1**) likely modulate the chemotactic coefficient of the evolved strains[28]. In other words, differing efficiency of chemotaxis and motility may account for the differences in swim ring diameters. To test this alternative hypothesis, we carried out single-cell measurements of motility through phase-contrast microscopy and single-particle tracking, for the ancestor as well as each of the evolved strains. We performed these experiments with a single representative strain from each lineage, as the flagellar mutations observed across all strains in each lineage were identical (**Fig 3**C). We observed that a majority of the cells in some of these populations were non-motile, and hence calculated the fraction of motile cells for each of the experimental replicates (**Fig 5**A). This suggests that the motile cells form the swim rings on motility plates while leaving a majority (non-motile cells) behind. We reconfirmed that the motile cells, likely at the leading edge of the swimming ring, were indeed fully resistant to $\chi$, for each of the strains tested in this experiment (**Fig S2**). For the motile cells, we calculated the distributions of swimming speed (**Fig 5**B) and tumble bias (**Fig 5**C). We observed that cells of the strains that displayed smaller swim diameter than ancestor (lineages 3, 5, 6, 7, 8, and 9) swam slower than the ancestor (**Fig 5**B). Whereas, the swimming speeds of the rest of the lineages (1, 2, and 10) were comparable to the ancestor (**Fig 5**B). The tumble bias for every evolved lineage was higher as compared to the ancestor, except in case of evolved lineage 1 (**Fig 5**C).

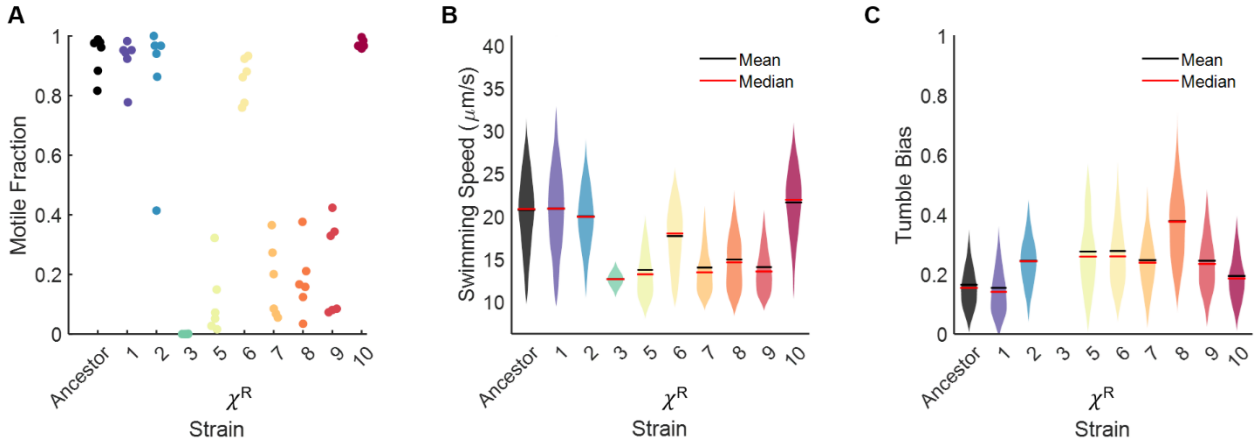


**Fig 5. Motile fraction, swimming speed, and tumble bias of evolved strains differ from those of the ancestors. (A)** Motile fraction calculated for each replicate experiment are indicated for each strain. **(B)** Distribution of single-cell swimming speeds for are plotted for each strain. **(C)** Tumble bias distributions of single cells are indicated for each strain (except $\chi$-resistant strain 3, where the motile fraction was negligible).

## Discussion

Flagellotropic phages are commonly found and have likely existed alongside bacteria in nature for billions of years of evolution[5,13,29–33]. Motile bacteria must frequently encounter flagellotropic phages. However, the evolutionary mechanisms of bacterial resistance to these phages are rarely studied. We examined the genetic and phenotypic consequences of the evolution of a model bacterium, *E. coli*, when repeatedly subjected to model flagellotropic phage, $\chi$. Instead of using the well-mixed environment of a shaking culture-flask, typical in phage-bacteria evolution assays, we challenged the bacteria to spatial confinement in swim plates, applying both motility constraints and evolutionary pressure from $\chi$. This approach selected for the bacteria to remain motile for nutrient acquisition and allowed us to monitor their motility.

$\chi$ is known to infect both *E. coli* and *Salmonella enterica*[14,34]. Our results suggest that the outermost D3 domain of *E. coli* flagellin serves as a binding pocket for phage $\chi$ (**Fig 3**B). This is intriguing because in *S. enterica*, which has a closely related chemotaxis and motility system, a mutant screen revealed a binding pocket for the same phage in the D2 domain- the same study also ruled out any involvement of the D3 domain in the interaction[35]. As reviewed by Beatson and coworkers, the D0 and D1 domains of the flagellin are relatively well conserved whereas the D2 and D3 are variable or hyper-variable[36]. This may suggest a strategy where $\chi$ evolved to target different variable domains in *Salmonella* and *E. coli*.

Some of our populations also featured mutations in genes involved in the synthesis or regulation of outer structures such as lipopolysaccharides (LPS) and capsules. For instance, one lineage had a significant (>70% frequency) mutation in the LPS-related gene *waaQ* at passages 5 and 10 (**Fig S1**). The gene encoding phosphotranferase RcsD (involved in capsular polysaccharide synthesis) also showed a mutation at >70% frequency at passage 10 in one lineage (**Fig S1**). LPS-related genes were similarly selected in an earlier study imposing $\chi$ pressure on *E. coli*[18]. Additionally, flagellotropic phage 7-7-1 uses LPS as the secondary receptor to infect soil bacterium *Agrobacterium* sp.[30]. Model coliphage T4 also uses LPS as a co-receptor[37,38]. Our results suggest the possibility that $\chi$ may also use LPS in some capacity during the adsorption and genome injection processes.

As discussed above, *S. enterica*, also susceptible to $\chi$, shares an almost identical chemotaxis and motility machinery with *E. coli*[39]. After reaching the *Salmonella* cell body by binding to the flagella, $\chi$ uses the AcrABZ-TolC efflux pump as a receptor to inject its genome[34]. One of the important functions of efflux pumps is the active removal of certain antibiotics if they enter the cell. Phages binding to the efflux pumps represent interesting therapeutic potential since resistance against such phages may occur through deletion of efflux pump, thus re-sensitizing the host cells to antibiotics[1,40]. Interestingly, we did not observe any mutations in the genes encoding these efflux pumps in our *E. coli* lineages evolved against $\chi$. It is possible that $\chi$ uses the efflux pump to inject its genome in *E. coli*, but the binding-related mutations in the flagellum were sufficient to resist $\chi$-attack. To test this hypothesis, we used a *tolC* knockout and tested if cells of this strain can swim through concentrated spots of $\chi$ on swim plates. We observed that while cells of our construct Δ*tolC* are slower than the WT strain, they are still susceptible to $\chi$ (**Fig S3**). Thus, we did not find strong evidence for any involvement of the TolC efflux pump in $\chi$ infection of *E. coli* cells.

In the nut-and-bolt model of $\chi$-attachment to the flagellum, the single tail fiber of $\chi$ fits the grooves formed by helically arranged flagellar monomers[14]. Rotation of the flagellum in the counter-clockwise direction, as viewed from the distal end, forces the phage to follow the grooves and translocate towards the cell body, similar to a nut following the threads of a bolt. In this model, clockwise rotation of the flagellum would result in the phage moving away from the cell[14]. The run-tumble motion of *E. coli* cells results from switching between counterclockwise and clockwise flagellar rotation, which causes runs and tumbles, respectively[39]. *E. coli* cells predominantly rotate counter-clockwise, resulting in more runs than tumbles[8,39]. Therefore, $\chi$-infection utilizes the more frequent counter-clockwise direction of flagellar rotation. Our single-cell tracking experiments

revealed that the tumble bias of all our evolved, $\chi$-resistant lineages increased, indicating a higher fraction of clockwise (tumble-inducing) flagellar rotation.

Antibiotic-resistant bacterial strains often have mutations in 16S and 23S rRNA genes, as these are common targets of antibiotics[41–43]. Recent evidence suggests that phage-resistance may also induce mutations in these regulatory genomic regions[44]. We observed mutations in the genes encoding 16S and 23S rRNA regions of several $\chi$-resistant mutants (**Fig S1**). This finding suggests that phage-resistance may also influence the effects of certain antibiotics on cells.

The century-old approach of using phages as therapeutics is experiencing a resurgence due to the rise in antibiotic-resistant bacterial infections[4]. Evolutionary trade-offs can be leveraged to our advantage in therapy[1]. However, trade-ups may also occur, potentially making the target bacterium more pathogenic[21]. Because motility is a fitness or virulence factor in several bacterial species[12], flagellotropic phages represent exciting therapeutic options[5]. Our observations suggest that bacteria evolving against phage $\chi$ lose motility in the early stages of evolution. This trade-off between phage resistance and motility could be advantageous, as it reduces bacterial fitness or virulence. The remaining bacteria can be eliminated by the immune system or with antibiotic-co-therapy. Thus, the early stages of bacterial evolution are relevant when considering therapeutic setting.

Later stages of bacterial evolution against the same phage represent more of an ecological setting where bacteria may encounter an environment rich in phages. To survive and potentially escape such an environment, bacteria may need to develop resistance to flagellotropic phages while retaining motility. In our study-system of *E. coli* and $\chi$-phage, this was achieved through mutations in the flagellar filament. Thus, our results provide insights into the evolutionary dynamics of motile bacteria interacting with flagellotropic phages.

# Materials and Methods

## Bacteria and phage strains

MG1655 was used as the wildtype (WT) ancestor strain, which was obtained from J. Wertz at the Coli Genetic Stock Center (CGSC) at Yale University, now re-branded as *E. coli* Genetic Resource Center (https://ecgrc.net/). *Salmonella*-infecting $\chi$-phage was obtained from Kelly Hughes at the University of Utah and grown on the permissive (Δ*recA*) strain BW25113 to change its methylation signature to *E. coli*.

The Δ*fliC* mutant of MG1655 was generated through P1-tranduction, replacing the *fliC* gene with a Kanamycin cassette. The Y246D amino acid substitution ($fliC^{Y246D}$) was made on the

isolated *fliC* gene via site-directed mutagenesis by substituting T at nucleotide position 736 with a G. The unmodified (*fliC*$^{WT}$) or modified (*fliC*$^{Y246D}$) flagellin was then cloned onto pTrc99A using XbaI and SalI enzymes. 100 µg/mL ampicillin and 20 µM IPTG were added to the cultures and plates when growing these strains.

## Growth protocols

Tryptone Broth (TB; 10 g tryptone, 5 g NaCl per L) was used for liquid cultures, 1.5% agar plates, 0.5% top agar for the double-layer method of phage propagation and 0.3% swim agar for swim plate assays. Overnight cultures were initiated from colonies grown on solid (1.5%) TB agar and placed into TB liquid medium, incubated with shaking (150 RPM) at 30°C. Bacterial stocks were stored in 25% glycerol at -80°C. High-titer stocks (lysates) of phages were grown by mixing a virus with its wildtype host bacteria in liquid broth and incubating for 12-24 hours as described above to allow phage population growth, followed by centrifugation and filtration (0.22 µm) to remove bacteria and obtain a cell-free lysate. Phages were enumerated (plaque-forming units [PFU] per mL) using the standard double-layer agar method where viruses form visible plaques on confluent lawns of wildtype host bacteria within 0.5% top agar, overlayed on 1.5% agar in the bottom layer.

## Isolation of Bacteria from Evolution Experiment

At least two individual isolates were obtained from each lineage at passage 10. The frozen stock was streaked out on 1.5% agar plates to obtain isolated colonies. Individual isolated colonies were picked and re-streaked onto fresh plates. Individual colonies from the second (doubly-isolated) plate were used for experiments with the isolates (**Fig 3**, **Fig 4**).

## Sequencing and mutant calling analysis

For whole genome sequencing of each lineage at passages 5 and 10, 200 µL of the frozen stock was used as an inoculum for 5 mL overnight cultures. For, cells were grown in TB overnight and a pellet after centrifugation of 1 mL culture was sent to SeqCenter who extracted the genome and prepared genomic DNA libraries and performed Illumina sequencing (paired-end reads of 151 bp length collected to a final coverage of ~100-fold across the reference genome). Mutant calling analysis was performed using breseq with default mode[18].

## Bacterial growth rate measurements

Overnight cultures of isolates were grown in in TB medium and then transferred to fresh TB in 200 µL total volumes (1 µL overnight culture into 199 µL fresh TB). Measurements were made in triplicate for isolate and their positions were randomized on the 96-well plate using

platedesigner.net. Cultures were incubated at 30 °C with shaking, and optical density (600 nm excitation) was monitored at 10-min intervals for 24 h by a BioTek Synergy H1 microplate reader. The growth rate was calculated by obtaining an exponential fit for the $OD_{600}$ values over time for each strain in the region where $\log(OD_{600})$ versus time is linear.

### Single-cell tracking experiments

Overnight cultures were grown in TB medium (30 °C), diluted 1:100 in fresh TB and re-grown for 4 hours at 30 °C, reaching the exponential phase of growth ($OD_{600}$ ~ 0.4-0.5). Exponential-phase cells were diluted into Motility Buffer (MB: 0.01 M potassium phosphate, 0.067 M NaCl, 0.1 mM EDTA, 1 μM methionine, 10 mM lactic acid) to $OD_{600}$ ~ $10^{-4}$ and allowed to equilibrate (chemotactically adapt to MB) at room temperature for 20 minutes before experiments. Cells were then introduced to an imaging chamber made by sticking #1.5 coverslips to glass slides via double-sided sticky tape. Both glass slides and coverslips were freshly cleaned (on the same day) with vacuum gas plasma to make their surfaces hydrophilic, thereby preventing adhesion of cells to these surfaces. After introducing the sample, the chamber was sealed on both sides with VALAP (equal parts Vaseline, lanolin, and paraffin wax) to prevent flows. Swimming cells were visualized at 30 °C with a Nikon Ti-E inverted microscope using a CFI Plan Fluor 4X/0.13 NA objective and PhL ring for phase-contrast. The cells were analyzed in MATLAB using a routine described previously[25,45].

### Calculation of motile fraction

Distributions of the swimming speed featured a peak ~ 5 μm/s. Performing the same experiments with MG1655 Δ*fliC* strain confirmed this peak to be due to non-motile cells (**Fig S4**). This peak terminated at 8-10 μm/s. Hence, cells with speed < 10 μm/s were identified as non-motile cells and the fraction of trajectories with speed > 10 μm/s was calculated as the motile fraction for each experiment.

## Acknowledgements

We thank Kelly Hughes for gifting us a stock of phage $\chi$ and John Wertz for his help in generating the *fliC* knockout for this work. We thank members of the Paul Turner Lab, Jeremy Moore, Lam Vo, Fotios Avgidis, Jake Sumner, and other members of the Yale Quantitative Biology Institute for interesting discussions and valuable feedback about this work. This study was funded by Yale University through Yale Center for Phage Biology and Therapy. TE acknowledges support from NIH (R01GM106189-09). JDA and PET acknowledge funding support from Howard Hughes Medical Institute Emerging Pathogens Initiative grant.

## References


1. Oromí-Bosch, A., Antani, J. D. & Turner, P. E. Developing Phage Therapy That Overcomes the Evolution of Bacterial Resistance. *Annu. Rev. Virol.* **10**, null (2023).
2. Koskella, B. & Brockhurst, M. A. Bacteria–phage coevolution as a driver of ecological and evolutionary processes in microbial communities. *Fems Microbiol. Rev.* **38**, 916–931 (2014).
3. Nobrega, F. L. *et al.* Targeting mechanisms of tailed bacteriophages. *Nat. Rev. Microbiol.* **16**, 760–773 (2018).
4. Kortright, K. E., Chan, B. K., Koff, J. L. & Turner, P. E. Phage Therapy: A Renewed Approach to Combat Antibiotic-Resistant Bacteria. *Cell Host Microbe* **25**, 219–232 (2019).
5. Esteves, N. C. & Scharf, B. E. Flagellotropic Bacteriophages: Opportunities and Challenges for Antimicrobial Applications. *Int. J. Mol. Sci.* **23**, 7084 (2022).
6. Kearns, D. B. A field guide to bacterial swarming motility. *Nat. Rev. Microbiol.* **8**, 634–644 (2010).
7. Wong, G. C. L. *et al.* Roadmap on emerging concepts in the physical biology of bacterial biofilms: from surface sensing to community formation. *Phys. Biol.* **18**, 051501 (2021).
8. Antani, J. D. *et al.* Mechanosensitive recruitment of stator units promotes binding of the response regulator CheY-P to the flagellar motor. *Nat. Commun.* **12**, 5442 (2021).
9. Chawla, R., Gupta, R., Lele, T. P. & Lele, P. P. A Skeptic's Guide to Bacterial Mechanosensing. *J. Mol. Biol.* **432**, 523–533 (2020).
10. Colin, R., Ni, B., Laganenka, L. & Sourjik, V. Multiple functions of flagellar motility and chemotaxis in bacterial physiology. *FEMS Microbiol. Rev.* **45**, fuab038 (2021).
11. Cremer, J. *et al.* Chemotaxis as a navigation strategy to boost range expansion. *Nature* **575**, 658–663 (2019).
12. Matilla, M. A. & Krell, T. The effect of bacterial chemotaxis on host infection and pathogenicity. *FEMS Microbiol. Rev.* **42**, fux052 (2018).
13. Gambino, M. & Sørensen, M. C. H. Flagellotropic phages: common yet diverse host interaction strategies. *Curr. Opin. Microbiol.* **78**, 102451 (2024).
14. Samuel, A. D. T. *et al.* Flagellar determinants of bacterial sensitivity to χ-phage. *Proc. Natl. Acad. Sci. U. S. A.* **96**, 9863–9866 (1999).
15. Ravid, S. & Eisenbach, M. Correlation between bacteriophage chi adsorption and mode of flagellar rotation of Escherichia coli chemotaxis mutants. *J. Bacteriol.* **154**, 604–611 (1983).
16. Schavemaker, P. E. & Lynch, M. Flagellar energy costs across the tree of life. *eLife* **11**, e77266 (2022).

17. Chevance, F. F. V. & Hughes, K. T. Coordinating assembly of a bacterial macromolecular machine. *Nat. Rev. Microbiol.* **6**, 455–465 (2008).
18. Deatherage, D. E. & Barrick, J. E. Identification of Mutations in Laboratory-Evolved Microbes from Next-Generation Sequencing Data Using breseq. in *Engineering and Analyzing Multicellular Systems: Methods and Protocols* (eds. Sun, L. & Shou, W.) 165–188 (Springer, New York, NY, 2014). doi:10.1007/978-1-4939-0554-6_12.
19. Yonekura, K., Maki-Yonekura, S. & Namba, K. Complete atomic model of the bacterial flagellar filament by electron cryomicroscopy. *Nature* **424**, 643–650 (2003).
20. Alvi, S. *et al.* Flagellar point mutation causes social aggregation in laboratory-adapted Bacillus subtilis under conditions that promote swimming. *J. Bacteriol.* **206**, e00199-24 (2024).
21. Burmeister, A. R. & Turner, P. E. Trading-off and trading-up in the world of bacteria–phage evolution. *Curr. Biol.* **30**, R1120–R1124 (2020).
22. Frank, S. A. *Microbial Life History: The Fundamental Forces of Biological Design*. (Princeton University Press, 2022).
23. Phan, T. V. *et al.* Direct measurement of dynamic attractant gradients reveals breakdown of the Patlak–Keller–Segel chemotaxis model. *Proc. Natl. Acad. Sci.* **121**, e2309251121 (2024).
24. Mattingly, H. H. & Emonet, T. Collective behavior and nongenetic inheritance allow bacterial populations to adapt to changing environments. *Proc. Natl. Acad. Sci.* **119**, e2117377119 (2022).
25. Vo, L. *et al.* Nongenetic adaptation by collective migration. *Proc. Natl. Acad. Sci.* **122**, e2423774122 (2025).
26. Liu, W., Tokuyasu, T. A., Fu, X. & Liu, C. The spatial organization of microbial communities during range expansion. *Curr. Opin. Microbiol.* **63**, 109–116 (2021).
27. Mattingly, H. & Emonet, T. A rule from bacteria to balance growth and expansion. *Nature* **575**, 602–603 (2019).
28. Arumugam, G. & Tyagi, J. Keller-Segel Chemotaxis Models: A Review. *Acta Appl. Math.* **171**, 6 (2020).
29. Guerrero-Ferreira, R. C. *et al.* Alternative mechanism for bacteriophage adsorption to the motile bacterium Caulobacter crescentus. *Proc. Natl. Acad. Sci.* **108**, 9963–9968 (2011).
30. Gonzalez, F., Helm, R. F., Broadway, K. M. & Scharf, B. E. More than Rotating Flagella: Lipopolysaccharide as a Secondary Receptor for Flagellotropic Phage 7-7-1. *J. Bacteriol.* **200**, e00363-18 (2018).
31. Ostenfeld, L. J. *et al.* A hybrid receptor binding protein enables phage F341 infection of Campylobacter by binding to flagella and lipooligosaccharides. *Front. Microbiol.* **15**, (2024).

32. Hardy, J. M. *et al.* The architecture and stabilisation of flagellotropic tailed bacteriophages. *Nat. Commun.* **11**, 3748 (2020).
33. Phothaworn, P. *et al.* Characterization of Flagellotropic, Chi-Like Salmonella Phages Isolated from Thai Poultry Farms. *Viruses* **11**, 520 (2019).
34. Esteves, N. C., Porwollik, S., McClelland, M. & Scharf, B. E. The Multidrug Efflux System AcrABZ-TolC Is Essential for Infection of Salmonella Typhimurium by the Flagellum-Dependent Bacteriophage Chi. *J. Virol.* **95**, 10.1128/jvi.00394-21 (2021).
35. Esteves, N. C., Bigham, D. N. & Scharf, B. E. Phages on filaments: A genetic screen elucidates the complex interactions between Salmonella enterica flagellin and bacteriophage Chi. *PLOS Pathog.* **19**, e1011537 (2023).
36. Beatson, S. A., Minamino, T. & Pallen, M. J. Variation in bacterial flagellins: from sequence to structure. *Trends Microbiol.* **14**, 151–155 (2006).
37. Yu, F. & Mizushima, S. Roles of lipopolysaccharide and outer membrane protein OmpC of Escherichia coli K-12 in the receptor function for bacteriophage T4. *J. Bacteriol.* **151**, 718–722 (1982).
38. Washizaki, A., Yonesaki, T. & Otsuka, Y. Characterization of the interactions between Escherichia coli receptors, LPS and OmpC, and bacteriophage T4 long tail fibers. *MicrobiologyOpen* **5**, 1003–1015 (2016).
39. Berg, H. C. *E. Coli in Motion*. (Springer New York, NY, 2004).
40. Burmeister, A. R. *et al.* Pleiotropy complicates a trade-off between phage resistance and antibiotic resistance. *Proc. Natl. Acad. Sci.* **117**, 11207–11216 (2020).
41. Sigmund, C. D., Ettayebi, M. & Morgan, E. A. Antibiotic resistance mutations in 16S and 23S ribosomal RNA genes of Escherichia coli. *Nucleic Acids Res.* **12**, 4653–4663 (1984).
42. Miyazaki, K. & Kitahara, K. Functional metagenomic approach to identify overlooked antibiotic resistance mutations in bacterial rRNA. *Sci. Rep.* **8**, 5179 (2018).
43. Depardieu, F. & Courvalin, P. Mutation in 23S rRNA Responsible for Resistance to 16-Membered Macrolides and Streptogramins in Streptococcus pneumoniae. *Antimicrob. Agents Chemother.* **45**, 319–323 (2001).
44. Zhou, W. *et al.* Genomic Changes and Genetic Divergence of Vibrio alginolyticus Under Phage Infection Stress Revealed by Whole-Genome Sequencing and Resequencing. *Front. Microbiol.* **12**, (2021).
45. Mattingly, H. H., Kamino, K., Machta, B. B. & Emonet, T. Escherichia coli chemotaxis is information limited. *Nat. Phys.* **17**, 1426–1431 (2021).

# Supplementary Information

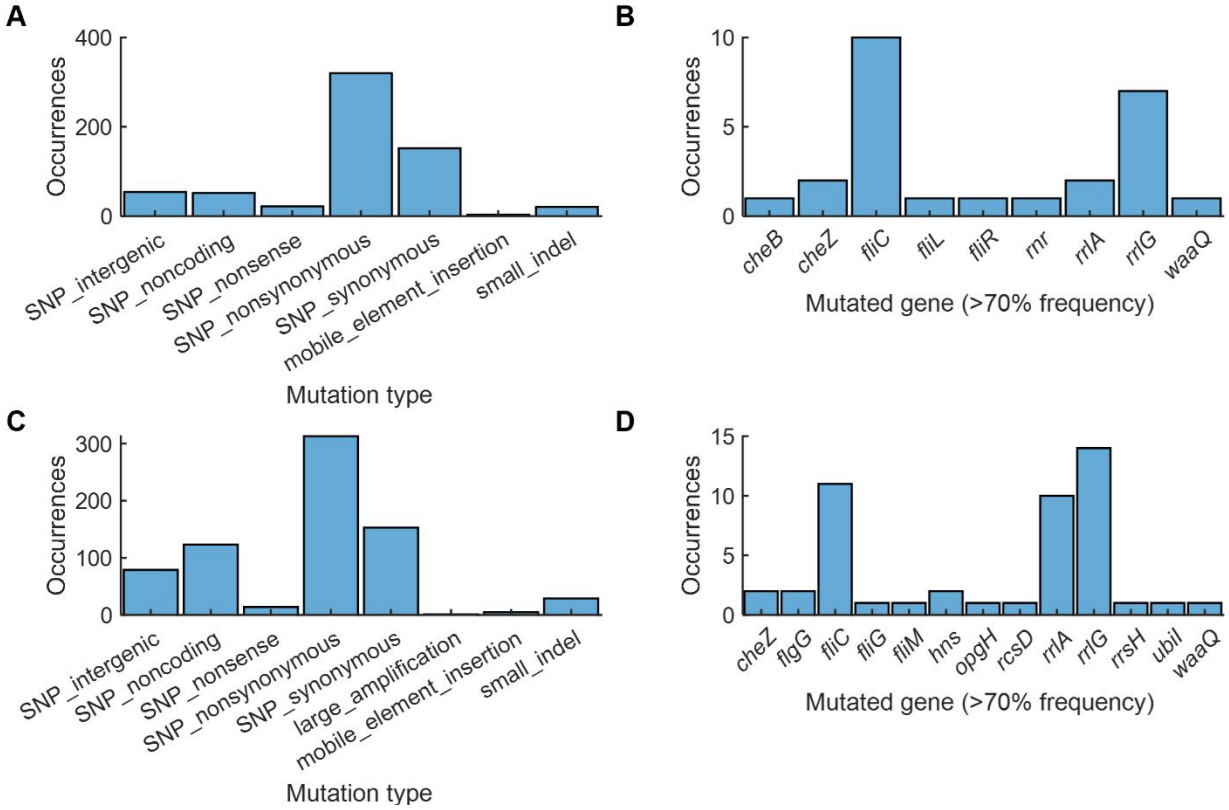


**Fig S1. Mutation frequencies in pooled genomes from all lineages (A, B) or all lineages except lineage 4 (C,D) are depicted. (A)** Number of occurrences of each type of mutation in passage 5. **(B)** Among mutations in passage 5 with frequency >70%, the number of occurrences of each gene are plotted. **(C)** Number of occurrences of each type of mutation in passage 10. **(D)** Among mutations in passage 10 with frequency >70%, the number of occurrences of each gene are plotted.

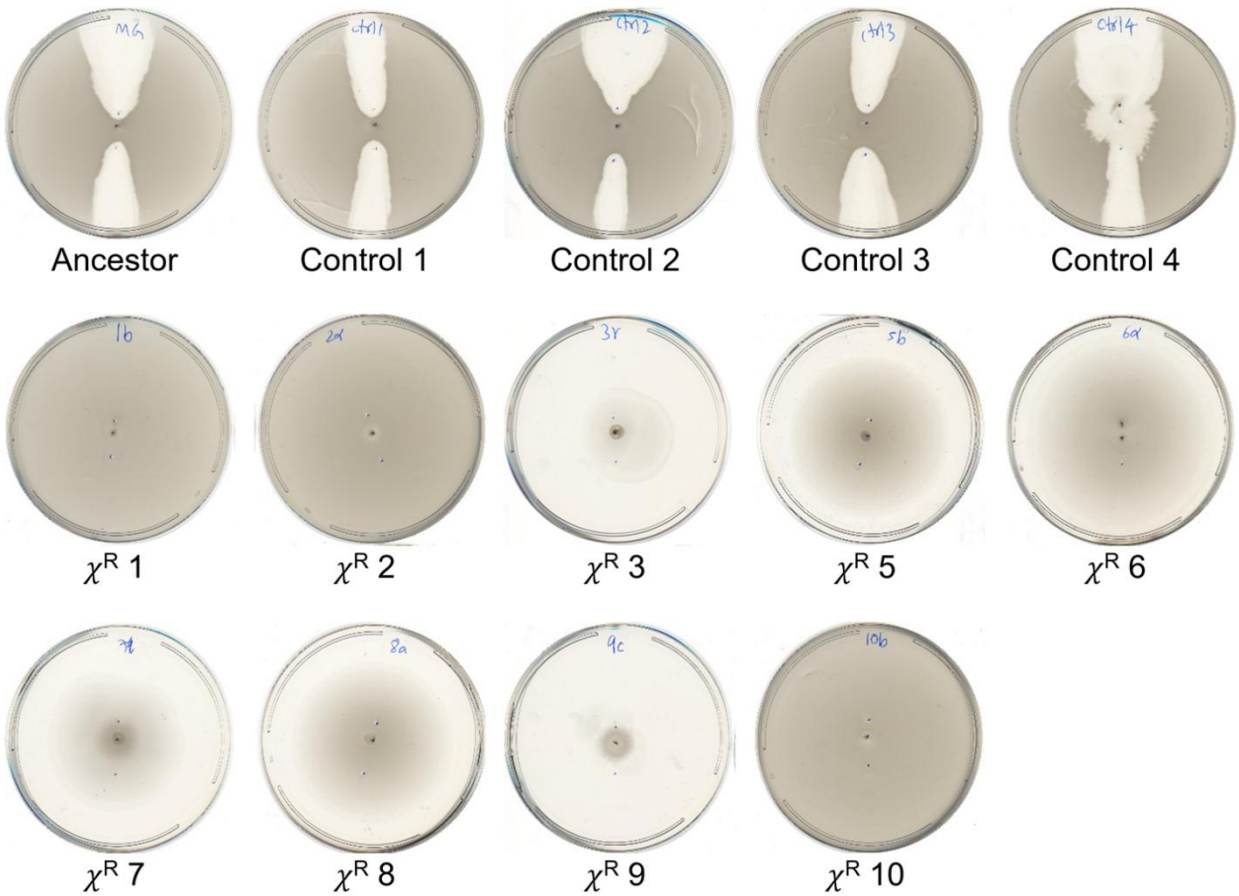


**Fig S2. Experiments to confirm that all isolates from passage 10 were motile and resistant to $\chi$.** Highly concentrated drops of χ were deposited at the locations, slightly away from the bacterial inoculum spot, marked as blue dots.

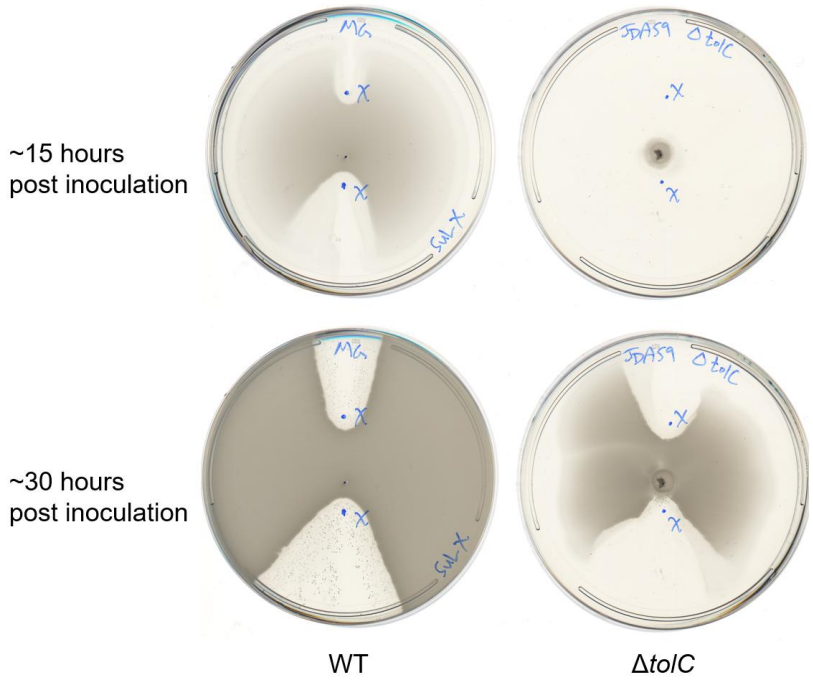


**Fig S3. Δ*tolC* cells expand slower than WT on swim plates but are susceptible to phage $\chi$.**

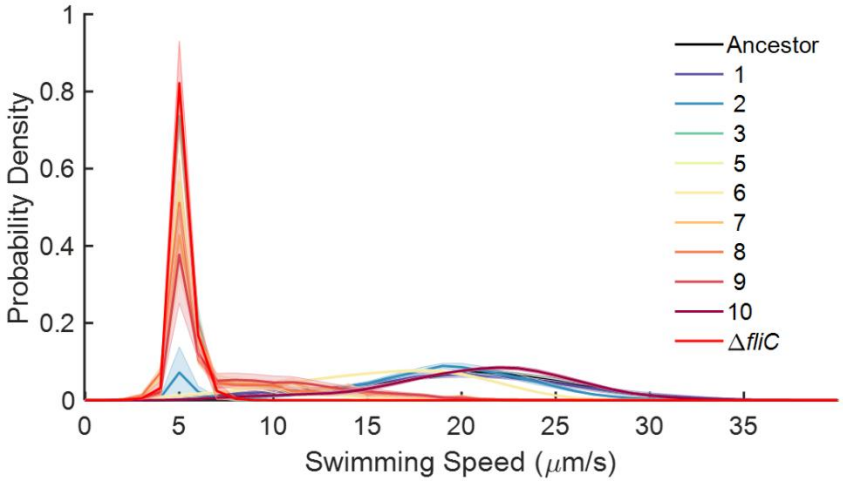


**Fig S4. Swimming speed distributions including both motile and non-motile cells.** The threshold for motile cells was determined using the MG1655 Δ*fliC* (flagellar filament knockout) strain. Based on the red distribution, we classified cells with swimming speed < 10 μm/s as non-motile.

**Table S1. Genes with mutation frequency >10% in passage 5.** Genes related to chemotaxis and flagellar motility are indicated in maroon color.

| Gene | Gene product |
|---|---|
| *ansB* | L-asparaginase 2 |

| | |
|---|---|
| *cheB* | protein-glutamate methylesterase/protein glutamine deamidase (chemotaxis receptor demethylation enzyme) |
| *cheZ* | chemotaxis protein CheZ |
| *cysW* | sulfate/thiosulfate ABC transporter inner membrane subunit CysW |
| *dcuC* | anaerobic C4-dicarboxylate transporter DcuC |
| *dmsA* | dimethyl sulfoxide reductase subunit A |
| *drpB/rseX* | cell division protein DrpB/small regulatory RNA RseX |
| *elfC* | putative fimbrial usher protein ElfC |
| *eutD* | phosphate acetyltransferase EutD |
| *flgH* | flagellar L-ring protein |
| *fliC* | flagellar filament structural protein |
| *fliL* | flagellar protein FliL |
| *fliO* | flagellar biosynthesis protein FliO |
| *fliR* | flagellar biosynthesis protein FliR |
| *flu* | self recognizing antigen 43 (Ag43) autotransporter |
| *gyrB* | DNA gyrase subunit B |
| *hemW* | heme chaperone HemW |
| *higA* | antitoxin/DNA-binding transcriptional repressor HigA |
| *insH8/yejO* | IS5 family transposase and trans-activator/adhesin-like autotransporter YejO |
| *kefC* | K(+) : H(+) antiporter KefC |
| *lysO/aqpZ* | L-lysine/thialysine exporter/water channel AqpZ |
| *manY* | mannose-specific PTS enzyme IIC component |
| *mutL* | DNA mismatch repair protein MutL |
| *narZ* | nitrate reductase Z subunit alpha |
| *opgH* | osmoregulated periplasmic glucans biosynthesis protein H |
| *pflA* | pyruvate formate-lyase activating enzyme |
| *rhsD* | protein RhsD |
| *rnr* | RNase R |
| *rpsO* | 30S ribosomal subunit protein S15 |
| *rrlA* | 23S ribosomal RNA |
| *rrlG* | 23S ribosomal RNA |
| *rrsH* | 16S ribosomal RNA |
| *rutE* | putative malonic semialdehyde reductase |
| *serS/dmsA* | serine--tRNA ligase/dimethyl sulfoxide reductase subunit A |
| *sgbU* | putative L-xylulose 5-phosphate 3-epimerase |
| *trpD* | anthranilate synthase subunit TrpD |
| *waaP* | lipopolysaccharide core heptose (I) kinase |
| *waaQ* | lipopolysaccharide core heptosyltransferase 3 |
| *yaiL* | DUF2058 domain-containing protein YaiL |
| *yajL* | protein/nucleic acid deglycase 3 |

| | |
|---|---|
| *ybeZ* | PhoH-like protein |
| *ybhG* | HlyD_D23 family protein YbhG |
| *ycfH* | putative metal-dependent hydrolase YcfH |
| *yfbP* | uncharacterized protein YfbP |
| *yfjD* | UPF0053 family inner membrane protein YfjD |
| *ygaP/stpA* | thiosulfate sulfurtransferase YgaP/DNA-binding transcriptional repressor StpA with RNA chaperone activity |
| *yhhX* | putative oxidoreductase YhhX |
| *yjeT* | DUF2065 domain-containing protein YjeT |
| *ynbD* | phosphatase domain-containing protein YnbD |
| *yobD* | DUF986 domain-containing inner membrane protein YobD |
| *yohP/dusC* | putative membrane protein YohP/tRNA-dihydrouridine(16) synthase |

**Table S2. Genes with mutation frequency >10% in passage 10.** Genes related to chemotaxis and flagellar motility are indicated in maroon color.

| Gene | Gene product |
|---|---|
| *bcp/hyfA* | thiol peroxidase/hydrogenase 4 component A |
| *cheB* | protein-glutamate methylesterase/protein glutamine deamidase (chemotaxis receptor demethylation enzyme) |
| *cheZ* | chemotaxis protein CheZ |
| *clpX* | ATP-dependent Clp protease ATP-binding subunit ClpX |
| *dnaG* | DNA primase |
| *fdnG* | formate dehydrogenase N subunit alpha |
| *fdnH* | formate dehydrogenase N subunit beta |
| *fecB* | ferric citrate ABC transporter periplasmic binding protein |
| *fecC* | ferric citrate ABC transporter membrane subunit FecC |
| *fepE* | polysaccharide co-polymerase family protein FepE |
| *flgG* | flagellar basal-body rod protein FlgG |
| *flgM/flgA* | anti-sigma factor for FliA (sigma(28))/flagellar basal body P-ring formation protein FlgA |
| *fliC* | flagellar filament structural protein |
| *fliD* | flagellar filament capping protein |
| *fliF* | flagellar basal-body MS-ring and collar protein |
| *fliG* | flagellar motor switch protein FliG |
| *fliL* | flagellar protein FliL |
| *fliM* | flagellar motor switch protein FliM |
| *fliT* | flagellar biosynthesis protein FliT |
| *ftsK* | cell division DNA translocase FtsK |
| *fumC* | fumarase C |
| *gcvT/yqfI* | aminomethyltransferase/protein YqfI |
| *glcB* | malate synthase G |

| | |
|---|---|
| *glgB* | 1,4-alpha-glucan branching enzyme |
| *gltP/yjcO* | glutamate/aspartate : H(+) symporter GltP/Sel1 repeat-containing protein YjcO |
| *hns* | DNA-binding transcriptional dual regulator H-NS (also involved in regulation of flagellar motility) |
| *hslO* | molecular chaperone Hsp33 |
| *hyfG* | hydrogenase 4 catalytic subunit HyfG |
| *kbp* | K(+) binding protein |
| *kdpC* | K(+) transporting P-type ATPase subunit KdpC |
| *kdpD* | sensor histidine kinase KdpD |
| *lacY* | lactose permease |
| *letB* | lipophilic envelope spanning tunnel |
| *metL* | fused aspartate kinase/homoserine dehydrogenase 2 |
| *metR* | DNA-binding transcriptional dual regulator MetR |
| *mnmC* | fused tRNA 5-aminomethyl-2-thiouridylate methyltransferase and tRNA 5-aminomethyl-2-thiouridylate synthase |
| *moaA* | GTP 3',8'-cyclase |
| *motA* | motility protein A |
| *murA* | UDP-N-acetylglucosamine 1-carboxyvinyltransferase |
| *murR* | DNA-binding transcriptional dual regulator MurR |
| *nanK* | N-acetylmannosamine kinase |
| *nuoH* | NADH:quinone oxidoreductase subunit H |
| *opgH* | osmoregulated periplasmic glucans biosynthesis protein H |
| *paaC* | phenylacetyl-CoA 1,2-epoxidase, structural subunit |
| *phnL* | methylphosphonate degradation complex subunit PhnL |
| *ppiC* | peptidyl-prolyl cis-trans isomerase C |
| *ptsP* | phosphoenolpyruvate-protein phosphotransferase PtsP |
| *radA* | DNA recombination protein |
| *rcnA* | Ni(2(+))/Co(2(+)) exporter |
| *rcsD* | RcsD phosphotransferase |
| *rho* | transcription termination factor Rho |
| *rhsC* | rhs element protein RhsC |
| *ribB/ubiK* | 3,4-dihydroxy-2-butanone-4-phosphate synthase/ubiquinone biosynthesis accessory factor UbiK |
| *rrfC* | 5S ribosomal RNA |
| *rrlA* | 23S ribosomal RNA |
| *rrlG* | 23S ribosomal RNA |
| *rrsH* | 16S ribosomal RNA |
| *rstB* | sensory histidine kinase RstB |
| *tdcE* | 2-ketobutyrate formate-lyase/pyruvate formate-lyase 4 |
| *tmcA* | tRNA(Met) cytidine acetyltransferase |
| *tyrS* | tyrosine--tRNA ligase |
| *ubiI* | 2-octaprenylphenol 6-hydroxylase |
| *waaQ* | lipopolysaccharide core heptosyltransferase 3 |

| | |
|---|---|
| *yadI* | putative PTS enzyme IIA component YadI |
| *yaiW* | surface-exposed outer membrane lipoprotein |
| *ybaT* | putative transporter YbaT |
| *ybbP* | putative ABC transporter membrane subunit YbbP |
| *ybcV/ybcW* | DUF1398 domain-containing protein YbcV/uncharacterized protein YbcW |
| *ycbZ/matP* | putative ATP-dependent protease YcbZ/macrodomain Ter protein |
| *ycgR* | flagellar brake protein YcgR |
| *ydeQ* | putative fimbrial adhesin protein YdeQ |
| *yecM/argS* | putative metal-binding enzyme YecM/arginine--tRNA ligase |
| *yeiQ* | putative oxidoreductase YeiQ |
| *yejK* | nucleoid-associated protein YejK |
| *ygeV* | putative sigma(54)-dependent transcriptional regulator YgeV |
| *yhaC/rnpB* | uncharacterized protein YhaC/RNase P catalytic RNA component |
| *yhbO* | protein/nucleic acid deglycase 2 |
| *yheS* | putative ATP-binding protein YheS |
| *yjjV* | putative metal-dependent hydrolase YjjV |
| *ynaM/uspF* | protein YnaM/universal stress protein F |
| *ynbD* | phosphatase domain-containing protein YnbD |
| *yncO/ydcC* | protein YncO/H repeat-associated putative transposase YdcC |
| *yqeB* | XdhC-CoxI family protein YqeB |
| *ytiE/yjiR* | protein YtiE/fused putative DNA-binding transcriptional regulator/putative aminotransferase YjiR |